Oligo(Cyclohexylidene)s and Oligo(Cyclohexyl)s as Bridges for Photoinduced Intramolecular Charge Separation and Recombination†

Wibren D. Oosterbaan,‡ Carola Koper,‡ Thijs W. Braam,‡ Frans J. Hoogesteger,‡ Jacob J. Piet,‡,|| Bart A. J. Jansen,‡ Cornelis A. van Walree,*,‡ H. Johan van Ramesdonk,§ Marijn Goes,§ Jan W. Verhoeven,§ Wouter Schuddeboom,|| John M. Warman,|| and Leonardus W. Jenneskens*,‡

Debye Institute, Department of Physical Organic Chemistry, Utrecht University, Padualaan 8, 3584 CH Utrecht, The Netherlands, Laboratory of Organic Chemistry, University of Amsterdam, Nieuwe Achtergracht 129, 1018 WS Amsterdam, The Netherlands, and Radiation Chemistry Department, IRI, Delft University of Technology, Mekelweg 15, 2629 JB Delft, The Netherlands

Received: October 9, 2002; In Final Form: February 14, 2003

A series of semirigid donor−bridge−acceptor (D−B−A) molecules was synthesized to study the effect of the position and number of nonconjugated olefinic bonds in the bridge on the photoinduced charge-separation and charge-recombination kinetics. The molecules consist of a phenylpiperidine electron donor, an oligo(cyclohexylidene) or oligo(cyclohexyl) bridge, and a dicyanovinyl acceptor. Partly saturated ter(cyclohexylidene) bridges were used as well. The edge-to-edge donor−acceptor separation of the compounds under study varies between 2.89 and 15.4 Å. The replacement of a C−C single bond by an olefinic bond increases the rate of charge separation with a factor of 3.0 ± 0.8 per replaced bond. For all D−B−A compounds the extended fully charge-separated state folds to a compact charge-transfer (CCT) conformer. The rate of charge recombination (CR) of the CCT state increases with solvent polarity for those compounds having an olefinic bond located three σ bonds from the acceptor. Thus, while in cyclohexane the CR rate is equal for all compounds, in benzene the CR rate in compounds with an olefinic bond near the acceptor is 10 times larger than in compounds with a single bond instead. It is believed that a (virtual) charge-transfer state involving the radical cation of the olefinic bond and the radical anion of the acceptor ($D-B^{\bullet+}-A^{\bullet-}$) is responsible for the enhanced CR process.

Introduction

Photoinduced long-range electron transfer (ET) has long been recognized as the key process in the conversion of solar energy to chemical energy as taking place in natural and artificial photosynthetic systems. The study of various donor−bridge−acceptor (D−B−A) molecules with rigid saturated hydrocarbon bridges has contributed significantly to the understanding of the electron-transfer process. The influence of factors as donor−acceptor separation, reaction medium, and free energy on the ET process has been studied extensively.[1−4] In the case of saturated hydrocarbon bridges, ET proceeds via a superexchange or through-bond mechanism[5] and its rate is related to the magnitude of the coupling between the locally excited donor or acceptor state and the charge-transfer (CT) state.

The observation that a bacteriochlorophyll (BChl) is located between the initially excited bacteriochlorophyll dimer (P) and the bacteriopheophytin (H) electron acceptor in the purple bacterial photosynthetic reaction center, combined with the fact that extremely fast ET from P to H occurs with a time constant[6] of 3 ps over a 17 Å center-to-center distance, has stimulated the research on the influence of intermediate π-systems on the rate of ET. It has been found that π-systems as well as other groups, such as a dihalocyclopropane unit,[7] which provide low energy virtual states $D^{\bullet+}-B^{\bullet-}-A$ or $D-B^{\bullet+}-A^{\bullet-}$, can enhance the rate of charge separation. Although a fast charge-separation step is beneficial for the efficiency of photochemical energy conversion, it should be realized that charge-recombination rates can be enhanced by super-exchange involving these states as well. For an extensive literature survey on the effect of intermediate and virtual states on charge-separation and -recombination rates the reader is referred to ref 8. π-Electron containing systems in a bridge may also participate in a so-called sequential mechanism[9,10] in which the $D^{\bullet+}-B^{\bullet-}-A$ or $D-B^{\bullet+}-A^{\bullet-}$ states exist as real intermediates.

An interesting bridge is represented by the oligo(cyclohexylidene) skeleton. Oligo(cyclohexylidene)s[11] (Chart 1A) consist of an array of cyclohexane rings which are linked at the 1 and/or 4 positions by double bonds. The $\sigma-\pi$-topology in these molecules is well capable of relaying through-bond interactions between functionalities attached to the termini as has been demonstrated[12,13] by photoelectron spectroscopy in combination with ab initio calculations. Self-assembled monolayers of α,ω-sulfur-functionalized oligo(cyclohexylidene)s have been applied as medium for electron transfer between CdSe quantum dots and a gold electrode.[14,15] The distance dependence of the rate of ET of these systems was found to be comparable to or in some cases even smaller than that[16,17] of fully π-conjugated bridges. In donor−acceptor-functionalized bi(cyclohexylidene) **D[3π3]A**, as well as in bi(cyclohexyl) **D[7]A** (Chart 2), photoinduced ET to a $D^{\bullet+}-B-A^{\bullet-}$ state has been observed.[18]

† "Oligo(cyclohexylidene)s" and "oligo(cyclohexyl)s" are shorthand notations for compounds named oligo(cyclohexan-1,4-diylidene)s and oligo(cyclohexan-1,4-diyl)s, respectively, according to IUPAC nomenclature.

‡ Debye Institute.

§ Laboratory of Organic Chemistry.

|| Radiation Chemistry Department.

10.1021/jp0271716 CCC: $25.00
Published on Web 04/04/2003

CHART 1: Oligo(cyclohexylidene)s (A) and Oligo(cyclohexyl)s (B) with the α- and *ω*-Positions Indicated

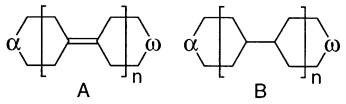

CHART 2: Structure of Donor−Bridge−Acceptor Compounds and Model Systems Studied

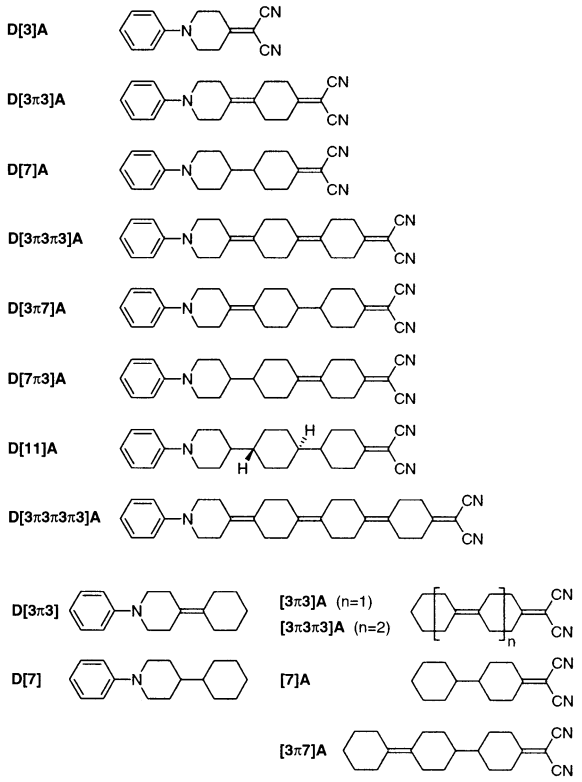

The donor **D** in these compounds is of the *N*,*N*-dialkylaniline type, while the acceptor **A** is a dicyanovinyl group. The part between brackets denotes the bond topology of the bridge. Although we were not able to determine the rate of charge separation, it was found that in benzene the rate of charge recombination in **D[3*π*3]A** is substantially (20 times) faster than that in **D[7]A**.[19] For **D[3*π*3]A** and **D[7]A** in the nonpolar solvent cyclohexane evidence was also obtained for the occurrence of large conformational changes (folding) accompanying charge separation in the nonpolar solvent cyclohexane. While for **D-[3*π*3]A** it could not be determined whether folding precedes or follows charge separation, in the case of **D[7]A** a harpooning mechanism,[20−23] in which charge separation precedes the folding process, was observed.

In the present study we report and discuss the photophysical properties of a series of longer D−B−A compounds **D[3*π*3*π*3]-A**, **D[7*π*3]A**, **D[3*π*7]A**, **D[11]A**, and **D[3*π*3*π*3*π*3]A** (Chart 2). In these compounds we have systematically varied the number and position of the olefinic bonds in the bridge as to be able to address the influence of these parameters on the charge-separation and -recombination processes. Furthermore, the photophysical properties of **D[3*π*3]A** and **D[7]A** are studied in more detail. In particular, the effect of solvent polarity on both the charge-recombination process and the folding process is discussed. The compounds were studied by means of steady-state spectroscopic methods and time-resolved absorption and fluorescence spectroscopy and microwave conductivity.

SCHEME 1: Synthetic Scheme for the Syntheses of D[3*π*3*π*3]A, D[3*π*3*π*3*π*3]A, D[7*π*3]A, D[11]A, and D[3*π*7]A[a]

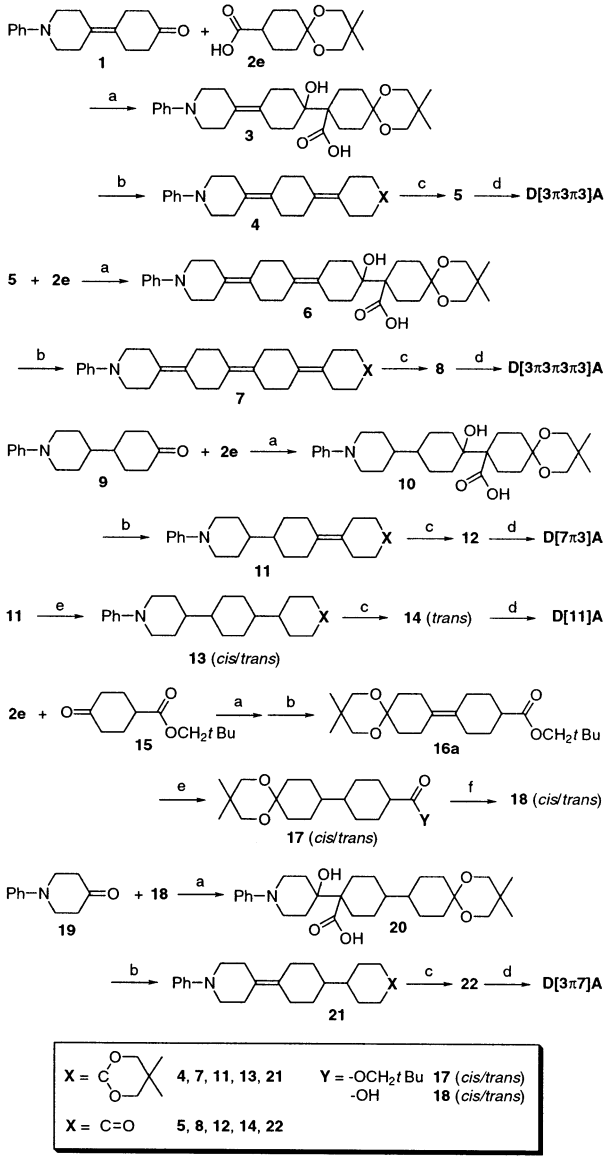

[a] Reagents: (a) (*i*-Pr)$_2$NLi, THF; (b) Me$_2$NCH(OCH$_2$CMe$_3$)$_2$, MeCN; (c) HCl, H$_2$O, THF; (d) H$_2$C(CN)$_2$, NH$_4$Ac, HOAc, benzene; (e) H$_2$, Pd/C, THF (EtOH); (f) 1. NaOH, H$_2$O 2. HCl, H$_2$O.

Results and Discussion

Synthesis. The syntheses of donor−bridge−acceptor compounds **D[3*π*3*π*3]A**, **D[3*π*7]A**, **D[7*π*3]A**, **D[11]A**, and **D-[3*π*3*π*3*π*3]A** are shown in Scheme 1. A key intermediate in the synthetic routes is carboxylic acid **2e**. Initially, it was prepared by a reaction sequence involving catalytic hydrogenation of ethyl 4-hydroxybenzoate to form ethyl 4-hydroxycyclohexanecarboxylate.[11,24] Since the yield of this step was irreproducible (0−95%), an alternative and more reliable route was used. This route (Scheme 2) involves the reaction of diethyl malonate with two equivalents of ethyl acrylate by 1,4-additions forming tetraethyl pentane-1,3,3,5-tetracarboxylate (**2a**), which was ring-closed by means of a Dieckmann condensation to form[25,26] triethyl 4-oxocyclohexane-1,1,3-tricarboxylate (**2b**). This product was converted into 4-oxocyclohexanecarboxylic acid (**2c**) by means of acidic hydrolysis and decarboxylation. Subsequently, **2c** was converted into **2e** via **2d**.

SCHEME 2: Synthetic Scheme for the Synthesis of 2c and 2e[a]

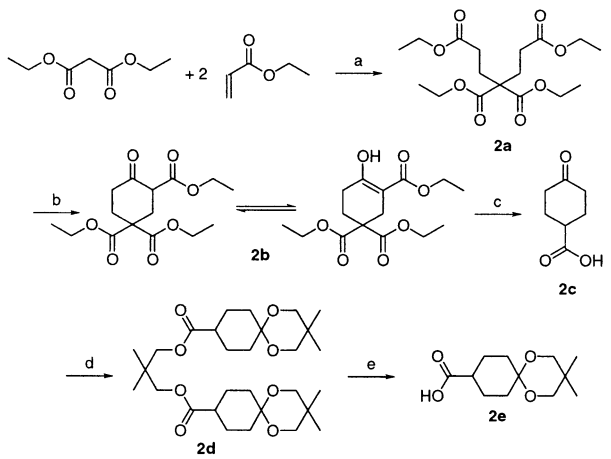

[a] Reagents: (a) EtONa, THF; (b) EtONa, diethyl ether; (c) HCl, H_2O; (d) 2,2-dimethyl-1,3-propanediol, H^+, toluene; (e) 1. NaOH, MeOH 2. HCl, H_2O.

Alkylation of the dianion of carboxylic acid **2e** with ketone **1** (Scheme 1) afforded β-hydroxy acid **3** which was decarboxylated and dehydrated to yield acetal **4**. Hydrolysis of **4** gave ketone **5**, which was condensated with malononitrile to afford **D[3π3π3]A**. The same reaction sequence starting from ketones **5** and **9** furnished D−B−A compounds **D[3π3π3π3]A** and **D-[7π3]A**, respectively. Catalytic hydrogenation of acetal **11** yielded **13** as a mixture of cis and trans isomers. Hydrolysis of this mixture followed by isomer separation gave the trans isomer of ketone **14**, which upon Knoevenagel condensation afforded **D[11]A**.

For the synthesis of **D[3π7]A**, synthon **18** was prepared as shown in Scheme 1. First, **16a** was prepared by coupling of the dianion of **2e** with **15**, which was prepared by esterification of 4-oxocyclohexanecarboxylic acid (**2c**, Scheme 2) with neopentyl alcohol. Dehydrative decarboxylation of the coupling product then yielded **16a** together with the byproducts **16b** and **16c** (see Supporting Information). Catalytic hydrogenation of **16a** gave the cis and trans isomers of **17** in a 1:1 ratio (according to GC analysis). Subsequent basic saponification followed by careful acidification gave **18** as a mixture of cis and trans isomers. For the synthesis of **D[3π7]A**, **18** had to be coupled to **19**. In this reaction it was found that the conditions under which dianion formation of carboxylic acid **2e** is readily achieved did not lead to dianion formation of **18**. This is probably caused by the low solubility of the dilithium salt of the dianion of **18** in THF. This solubility problem was solved by Trost and Tamaru[27] for a similar carboxylic acid by the use of THF−HMPA mixtures. Although we found that the addition of HMPA indeed promoted dianion formation of **18**, in our hands the best results were obtained by the use of TMEDA instead of HMPA. Dehydrative decarboxylation of **20**, followed by deprotection and condensation with malononitrile, finally gave **D[3π7]A**.

All D−B−A compounds possess high melting points and low solubilities in common organic solvents which decrease with increasing molecular size.

Ground-State Conformational Properties and Donor−Acceptor Distances. An important factor in the study of charge separation in D−B−A compounds is the distance between donor and acceptor, which should be well-defined. Therefore, rigid bridges, such as norbornyl[28] (see however ref 29), cubyl,[30] and steroid skeletons,[31,32] have been applied. The oligo(cyclohexylidene) and oligo(cyclohexyl) bridges used in the present study

Figure 1. Anti-syn-equilibrium of a bi(cyclohexylidene).

TABLE 1: Center-to-Center R_c and Edge-to-Edge R_e Donor−Acceptor Distances from MM2-Optimized Geometries of the D−B−A Compounds under Study[a]

compound		R_c (Å)	R_e (Å)
D[3]A		4.16	2.89
D[3π3]A	a	8.3	7.02
	a	[8.41]	[7.04]
	s	7.5	6.3
D[7]A		8.6	7.34
		[8.70]	[7.33]
D[3π3π3]A	aa	12.5	11.19
	as	11.7	10.52
	sa	11.5	10.45
	ss	11.6	10.36
D[3π7]A	a	12.6	11.39
	s	10.9	9.98
D[7π3]A	a	12.3	11.37
	s	11.2	10.05
D[11]A		13.1	11.84
D[3π3π3π3]A	aaa	16.7	15.37
	sss	15.4	14.24

[a] Distances between brackets are crystal data.[35] The labels "a" and "s" denote anti and syn geometry, respectively, with the first label referring to the double bond closest to the donor.

are expected to be considerably more flexible. For the bridges which contain an olefinic bond syn−anti isomerism (Figure 1) is important. For 4,4′-di-*tert*-butylbi(cyclohexylidene) under isomerization conditions an equilibrium composition with a anti/syn ratio of 0.83/0.17 has been reported[33] which corresponds to a Gibbs free energy difference of 0.95 kcal mol^{-1}. It is reasonable to expect that also for the compounds in the present study both syn and anti conformers are present in solution.

Support for the presence of different conformers in solution of the compounds with bridges that contain an olefinic bond was found[18] in ^{1}H NMR spectra of **D[3π3]A**, **D[3π3]**, and **[3π3]-A**. For these compounds a single, time-averaged chemical shift is observed for the equatorial and axial protons attached to the same carbon atom in the saturated hydrocarbon rings, whereas for **D[7]A**, **D[7]**, and **[7]A** distinct signals are observed for the equatorial and axial protons attached to the same carbon atom. This implies that compounds which contain an olefinic bond are conformationally flexible on the NMR time scale, while the conformation of their saturated analogues is frozen. Moreover, it was found that in **D[7]A** and **D[7]** the phenyl group occupies an equatorial position.[18] Nevertheless, B3LYP calculations on **D[3π3]** have shown[34] that a conformer with the phenyl ring in an axial position is sufficiently low in energy (0.8 kcal mol^{-1} above the energy minimum) to be accessible at room temperature. The donor−acceptor distance in this conformer is, however, only slightly different from that of the lowest energy conformer.

As a consequence of the occurrence of syn−anti isomerism (see Figure 1), the interchromophoric distance in the compounds with double bonds in the bridge is not fixed. To get an estimate of the variation in the interchromophoric distance molecular mechanics (MM2) calculations have been performed on all possible syn and anti conformers of the D−B−A compounds with bridges that contain one or more olefinic bonds. In Table 1 the donor−acceptor edge-to-edge distances R_e of the various D−B−A compounds and their syn and anti conformers (if any) are listed. The distance R_e is measured as the distance between

the anilino nitrogen atom and the olefinic C atom of the acceptor which is incorporated in the ring. As can be seen syn−anti interconversion produces a variation in the edge-to-edge distance of up to 1.4 Å (for **D[3π7]A**). In Table 1 also the center-to-center distance R_c has been indicated. This is the distance between the midpoint of the phenyl-C−N bond and the midpoint of the central olefinic bond of the acceptor. For **D[3π3]A** and **D[7]A** the calculated R_e and R_c values can be compared with their crystal structures.[35] In the crystal, the (partly) saturated six-membered rings of both molecules adopt a chair-type conformation and the phenyl group adopts a (pseudo) *equatorial* orientation. The bridge of **D[3π3]A** is in an anti conformation. As can be seen in Table 1 the MM2 distances are in good agreement with the crystal data.

Electronic Absorption Spectra. The absorption spectra of **D[3π3]A**, **D[7]A**, **D[3π3]**, **D[7]**, **[7]A**, and **[3π3]A** have been discussed before[18,34] and will only be briefly reviewed here. The *N*,*N*-dialkylanilino donor exhibits three absorption bands in the region 195−350 nm. For **D[7]** in cyclohexane, these bands are positioned at 203, 255 and 289 nm.[18] The olefinic bond in 1,1′-bi(cyclohexylidene) has a maximum at 206 nm,[36,37] while the $\pi^*\leftarrow\pi$-transition of the dicyanovinyl acceptor in **[7]A** gives rise to a single maximum at 235 nm.[18] In **[3π3]A**, besides these two $\pi^*\leftarrow\pi$-transitions, another band with a maximum at 274 nm in cyclohexane[18] is present, which has been ascribed to a transition involving charge transfer from the olefinic bond to the dicyanovinyl acceptor.[18,38]

The absorption spectrum of **D[7]A** can be described as the sum of the spectra of **D[7]** and **[7]A**. Hence, no noticeable ground-state interaction between the donor and acceptor in **D-[7]A** is present. The same was concluded[18] for **D[3π3]A**, but a careful reexamination of the absorption and excitation spectra of this compound revealed a very weak absorption tail extending to about 355 nm in cyclohexane (estimated band maximum between 300 and 320 nm). This absorption is neither present in **[3π3]A** nor in **D[3π3]** and is therefore ascribed to a transition involving charge separation from the phenylpiperidine donor to the dicyanovinyl acceptor: $D^{\bullet+}[3\pi3]A^{\bullet-} \leftarrow D[3\pi3]A$. It thus appears that the presence of the olefinic bond in **D[3π3]A** induces a ground-state interaction between the anilino donor and the dicyanovinyl acceptor. For **D[3]A**, which has an identical donor−acceptor pair, the position of the CT absorption has been reported to be located at 342 nm in *n*-hexane,[39,40] and it has a considerably larger absorption coefficient. Due to the larger distance between the charges, the CT state $D^{\bullet+}[3\pi3]A^{\bullet-}$ will be less stabilized than that of **D[3]A**, and hence a blue-shift for the absorption maximum is expected,[2] which is indeed observed.

The absorption spectra of **D[7π3]A**, **D[3π3π3]A**, **[3π3π3]-A**, and **D[3π3]** in dichloromethane are presented in Figure 2. Absorption maxima and molar absorption coefficients are tabulated in Table 2. The absorption spectrum of **[3π3π3]A** shows an absorption maximum which is slightly red-shifted as compared to that of **[3π3]A**. Furthermore, in **[3π7]A** CT absorption bands could not be detected. The absorption spectra of **D[3π3π3]A**, **D[7π3]A**, **D[3π7]A**, and **D[11]A** can be reasonably well described as the sum spectra of separate donor and acceptor compounds.

It is important to note that the UV spectra show that in the wavelength range 300−315 nm, in which most samples have been excited for fluorescence measurements, in the case of **D-[7]A**, **D[3π7]A**, and **D[11]A** only the anilino donor is excited, while in the case of **D[3π3]A**, **D[3π3π3]A**, and **D[7π3]A** only

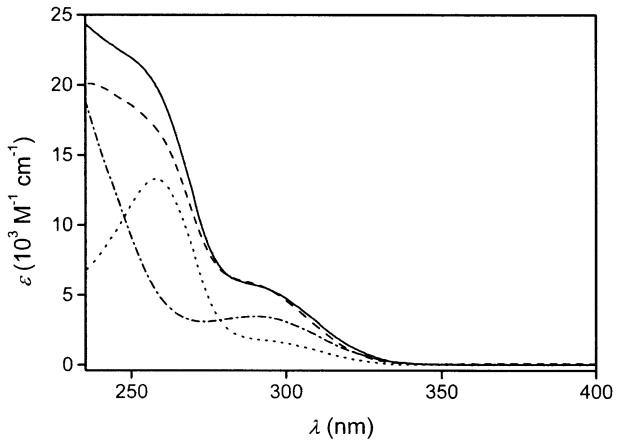

Figure 2. Absorption spectra of **D[3π3π3]A** (solid), **D[7π3]A** (dash), **[3π3π3]A** (dash−dot), and **D[3π3]** (dot) in dichloromethane at 20 °C.

TABLE 2: Absorption Maxima λ_{max} (nm) and Molar Absorption Coefficients ϵ (10^3 M^{-1} cm^{-1}) Determined in CH_2Cl_2 at 20 °C (range: 230−500 nm)

compound	λ_{max}	ϵ
D[3π3]	258.0	13.3
D[7]	258.5[a]	12.0
D[3π3]A	248.0	20.7
D[7]A	245.5[a]	21.1
[3π3]A	286.5	3.58
[3π3π3]A	290.5	3.47
[3π7]A	236.0	15.8
D[3π3π3]A		22.65[b]
D[7π3]A	236.0	20.1
D[3π7]A	244.5[a]	23.8
D[11]A	245.5[a]	22.2

[a] Shoulder in the region 285−295 nm. [b] Not any maximum present, ϵ at 245 nm.

about one-third of the absorbed excitation light will produce a locally excited donor and about two-thirds of the excitation light will produce a "local" $[3\pi^{\bullet+}3]A^{\bullet-}$ charge-transfer state. Starting with these two locally excited states, in principle two processes are possible: electron transfer, in which the electron residing on the excited donor is transferred to the acceptor, and hole transfer, in which the hole initially produced on an olefinic bond is transferred to the *N*,*N*-dialkylanilino donor. In **D[3π3]A** excitation in the 300−315 nm region will also directly produce the fully charge-separated state.

Solvent Dependence of the Steady-State Fluorescence of D[3π3]A and D[7]A. Fluorescence maxima ν_f and fluorescence quantum yields Φ_f of all D−B−A compounds as well as those of **[3π3]A** and **[3π3π3]A** are given in Table 3. The steady-state fluorescence spectra of **D[3π3]A** and **D[7]A**, recorded in solvents of different polarity, are presented in Figure 3. The local donor emission, located at 336 nm for both **D[3π3]** and **D[7]** in cyclohexane,[18] is largely quenched for **D[3π3]A** (≥99.8%) and **D[7]A** (≥97%) in all solvents.[41] A comparison between the emission spectra of **D[3π3]A** and those of **[3π3]A** (not shown) reveals that emission from the partly charge-separated state **$D[3\pi^{\bullet+}3]A^{\bullet-}$**, which is formed upon photoexcitation of **D[3π3]A** as well (see above), is not present in any solvent. This indicates that, in addition to electron transfer from the excited phenylpiperidine donor to the dicyanovinyl acceptor, also hole transfer from the olefinic bond to the phenylpiperidino donor takes place. The fluorescence bands which remain are ascribed to the fully charge-separated states **$D^{\bullet+}[3\pi3]A^{\bullet-}$** and **$D^{\bullet+}[7]A^{\bullet-}$** for **D[3$\pi$3]A** and **D[7]A**, respectively.[18]

TABLE 3: Experimental Steady-State Charge-Transfer Fluorescence Maxima ν_f (in nm) (Quantum Yield $\Phi_f/10^{-3}$) of the Compounds Given in Various Solvents at 20 °C Together with the Results of Solvatochromic Fits

solvent	Δf	D[3π3]A	D[7]A	[3π3]A	D[3π3π3]A	D[7π3]A	D[3π7]A	D[11]A	[3π3π3]A	D[3π3π3π3]A
cyclohexane	0.101	388 (3.0) 521 (32)	497[a] (28)	361 (1.2)	511 (48)	512 (18)	496 (27)	508 (4.7)	360 (2.0)	*b*
benzene[c]	0.117	525 (3.0)	515 (23)	416 (15)	574 (3.2)	576 (2.6)[d]	548 (3.9)	547 (1.8)	415 (22)	~415, 577[d]
di-*n*-pentyl ether	0.173	525[a](5.5)	483 (17)	378 (4.1)	550 (8.1)	550 (4.4)[d]	531 (4.5)	~500[a] (1.6)	379 (6.9)	*b*
di-*n*-butyl ether	0.193	520[a](4.7)	484 (17)	381 (4.8)	554 (6.2)	555 (3.5)[d]	534 (4.1)	518[a,d] (~1.7)	382 (7.2)	*b*
diisopropyl ether	0.234	522 (3.8)	521 (20)	389 (7.9)	558 (3.9)	566 (2.1)[d]	537 (2.6)	540[e] (0.5)	389 (9.2)	*b*
diethyl ether	0.254	542 (2.9)	545 (12)	409 (10)	576 (1.9)	578 (1.1)[d]	555 (1.9)	552 (1.2)	410 (14)	*b*
ethyl acetate	0.293	630	650	468 (8.1)	*f*	~468 (1.4)[g]	*f*	*f*	468 (9.9)	~468 (*b*)
THF	0.308	630 (0.3)	650	464 (12)	~635[a]	~464 (1.3)[g]	~650[a] (≤0.1)	*f*	465(13)	~465 (2.2)
CH_2Cl_2	0.319			461 (19)					461 (25)	
butyronitrile	0.376			512 (1.1)					512 (1.0)	
$\nu_f(0)$ (10^3 cm^{-1})		30.8 ± 0.5	28.9 ± 1.3	32.0 ± 1.0	20.7 ± 0.4	20.8 ± 0.3	22.5 ± 1.0	20.7 ± 0.3	32.0 ± 0.9	
slope (10^3 cm^{-1})		−49.3 ± 2	−43.9 ± 5	−32.5 ± 3.6	−13.0 ± 2.2	−13.8 ± 1.5	−12.5 ± 2.3	−9.6 ± 1.4	−32.6 ± 3.5	
correlation coefficient		0.997	0.974	0.959	0.958	0.982	0.954	0.989	0.961	

[a] Not used in the solvatochromic fit (see text). [b] Solubility too low. [c] Values obtained in benzene were not used in the solvatochromic comparison, since it is known that the polarity of benzene is not well described by its Δf. [d] Maximum obtained by deconvolution. [e] Value obtained by streak camera measurement. [f] No CT fluorescence observed. [g] Residual acceptor emission.

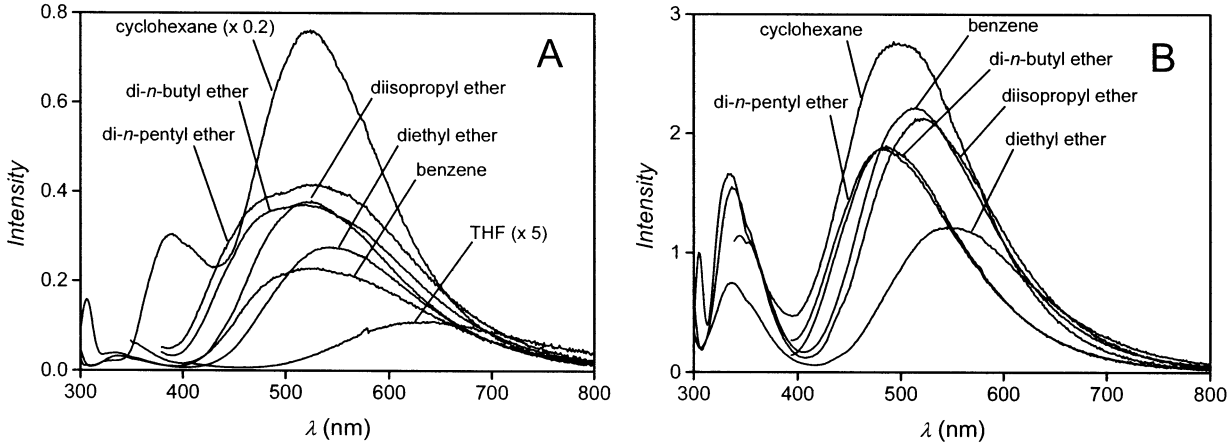

Figure 3. Fluorescence spectra of **D[3π3]A** (A) and **D[7]A** (B) in various solvents (excited between 270 and 300 nm). The intensity of all spectra is corrected for the absorbance (excited at 300 nm).

In cyclohexane, **D[3π3]A** clearly shows two CT bands positioned at 388 and 520 nm. The 520 nm band has previously been assigned to a folded or compact charge-transfer (CCT) conformer of the $D^{\bullet+}[3\pi3]A^{\bullet-}$ state.[18] The remaining band at 388 nm (3.20 eV) is assigned to the extended CT state (ECT state) of $D^{\bullet+}[3\pi3]A^{\bullet-}$.

The energy of the CT fluorescence is given by[2]

$$h\nu_f = \Delta G - \lambda_i' - \lambda_s + E_{00} \quad (1)$$

where h is Planck's constant, ΔG is the (negative) energy difference between the relaxed locally excited state and the relaxed CT state, λ_i' is the (positive) inner reorganization energy upon going from the Franck−Condon ground state formed upon CT fluorescence to the relaxed ground state, while λ_s is the solvent reorganization energy associated with this process. E_{00} is the zero−zero transition energy of the locally excited state from which charge transfer takes place. In a model where the donor and acceptor are represented by two spheres with mean radius r separated by a center-to-center distance R_c and immersed in a medium with refractive index n and permittivity ϵ_s eq 1 becomes[2]

$$h\nu_f = F[E_{ox}(\mathbf{D}) - E_{red}(\mathbf{A})] - e^2/37r - \lambda_i' + e^2(1/r - 1/R_c)(2/\epsilon_s - 1/n^2) \quad (2)$$

where F is Faraday's constant, e is the elementary charge, and $E_{ox}(\mathbf{D})$ and $E_{red}(\mathbf{A})$ are the oxidation and reduction potentials of donor and acceptor, respectively, as determined in acetonitrile ($\epsilon_s = 37$). When it is assumed that λ_i' is independent of R_c, which is reasonable since the main portion of the structural reorganization is expected to be located on the donor and acceptor sites and not on the bridge, eq 2 predicts a blue shift of the ECT emission maximum upon increasing R_c. For **D[3]A** in cyclohexane an emission maximum of 450 nm[40] (2.76 eV) has been reported and hence the ECT state $D^{\bullet+}[3\pi3]A^{\bullet-}$ of **D-[3π3]A** is indeed destabilized with respect to that of **D[3]A** by an amount of 0.44 eV.

While for **D[3π3]A** in cyclohexane two maxima are present, one corresponding to an ECT species and one to a CCT species, in the more polar solvents di-*n*-pentyl ether and di-*n*-butyl ether only a single very broad fluorescence band is present (Figure 3A). The full widths at half-height $\Delta\nu_{1/2}$ of the spectra in di-*n*-pentyl ether and di-*n*-butyl ether are ~7.4 and ~7.2 × 10^3 cm^{-1}, respectively, while values for CT fluorescence bands typically range from 4.5 to 6.5 × 10^3 cm^{-1}.[42] Furthermore, the location of the band maximum seems to be virtually independent of solvent polarity. These observations indicate that also in di-*n*-pentyl ether and di-*n*-butyl ether emission is observed from both ECT and CCT species. A similar broad band is present in benzene which shows that even in this quasi polar solvent CCT emission is observed. This supports our earlier presumption[18] that the small excited-state dipole moment obtained with time-resolved microwave conductivity (TRMC) in benzene is due to the presence of folded conformers. Note that the occurrence of two species in this solvent was confirmed with time-resolved

TABLE 4: Deconvolution of Fluorescence Spectra of D[3π3]A[a]

		ECT			CCT		
solvent	Δf	ν_{max}	$\Delta\nu$	b	ν_{max}	$\Delta\nu$	b
cyclohexane	0.100	25.62	4.74	−0.312	19.04	4.76	−0.122
di-*n*-pentyl ether	0.173	21.42	4.75[b]	−0.107	17.66	4.75[b]	−0.120
di-*n*-butyl ether	0.194	21.07	4.75[b]	−0.092	17.53	4.75[b]	−0.119
diisopropyl ether	0.237	19.11	5.56	−0.113			
diethyl ether	0.251	18.36	5.33	−0.090			
ethyl acetate	0.292	15.87	5.57	−0.021			

[a] Values for ν_{max} and $\Delta\nu$ are given in 10^3 cm^{-1}. [b] $\Delta\nu$ fixed at this value (see text).

fluorescence spectroscopy (see "Time-Resolved CT Fluorescence" section). The fluorescence spectra of **D[3π3]A** in diisopropyl ether, diethyl ether, ethyl acetate (not shown in Figure 3A), and THF have normal band shapes and widths. Bandwidths $\Delta\nu_{1/2}$ range from 5.34 to 5.57 × 10^3 cm^{-1}. On the basis of the electrostatic nature of the driving force for folding, less CCT emission is expected in these polar solvents and the band maxima are considered to be representative for the ECT species.

Since we were not able to distinguish between the emission of the extended and the compact CT conformers in di-*n*-pentyl ether and di-*n*-butyl ether, we deconvoluted[43] the steady-state spectra by skewed Gaussian functions:[44]

$$I(\nu) = f_{max} \exp(-\ln 2[\ln(1 + 2b(\nu - \nu_{max})/\Delta\nu)/b]^2) \quad (3)$$

The value for the full bandwidth at half-height $\Delta\nu_{1/2}$ is given by

$$\Delta\nu_{1/2} = (\Delta\nu \sinh b)/b \quad (4)$$

The value for $\Delta\nu$ was fixed at 4.75 × 10^3 cm^{-1}, i.e., close to the value obtained for the ECT and CCT bands in the cyclohexane spectrum (Table 4 and Figure 1S). The positions of the maxima for the ECT and CCT species obtained in this way fit well in the solvatochromic trend obtained by means of a Lippert−Mataga analysis (see below).[45]

The emission spectra of **D[7]A** are given in Figure 3B. It is immediately evident that the emission spectrum of **D[7]A** in cyclohexane is very broad, suggesting the presence of more than one emitting species. It was found by Hoogesteger et al. by means of nanosecond time-resolved emission measurements that in cyclohexane the emission initially appears at 440 nm and subsequently shifts to 500 nm, reflecting the conversion of an ECT into a CCT species.[18] These initial and final fluorescence maxima are indicated in Figure 4 by open circles. It appears that the initial maximum is red-shifted as compared to that of the ECT species of **D[3π3]A**. In the more polar solvents the emission bands have usual bandwidths [(5.1−5.7) × 10^3 cm^{-1}] with maxima that shift with solvent polarity. It is thought that these emission bands represent predominantly ECT emission.[46]

On the assumption that the excited-state dipole moment (μ_e) is large as that of the ground state, the Lippert−Mataga relationship[47] (eq 5) predicts a linear relationship between the fluorescence maximum ν_f of a CT state with dipole moment μ_e and the solvent polarity parameter Δf.

$$\nu_f = \nu_f(0) - \frac{2\mu_e^2}{hc\rho^3}\Delta f \quad (5)$$

$$\Delta f = \frac{\epsilon_s - 1}{2\epsilon_s + 1} - \frac{n^2 - 1}{4n^2 + 2} \quad (6)$$

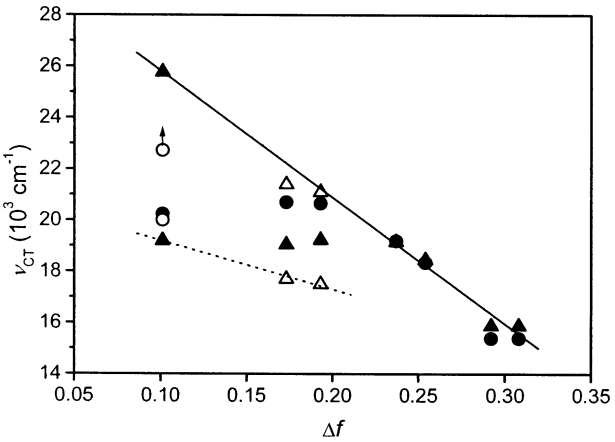

Figure 4. Plot of charge-transfer fluorescence maxima ν_f versus the solvent polarity parameter Δf: (▲) **D[3π3]A**; (△) maxima for **D[3π3]A** obtained by deconvolution of the experimental spectrum (eq 3). Note that these maxima have not been used in the Lippert−Mataga analysis: (●) **D[7]A**; (○) maxima derived from time-resolved data for **D[7]A**. The solid line is the fit for ECT emission of **D[3π3]A**; the dotted line is a guide to the eye for CCT emission of **D[3π3]A**.

In eqs 5 and 6, which are in CGS units, c is the velocity of light, and $\nu_f(0)$ the gas-phase position of ν_f. Furthermore, ρ denotes the effective radius of the solvent cavity enclosing the CT species.

In Figure 4 the fluorescence maxima ν_f found for **D[3π3]A** and **D[7]A** are plotted versus Δf. A good fit to eq 5 is obtained for the ECT emission maximum of **D[3π3]A** in cyclohexane and the emission maxima in diisopropyl ether and more polar solvents. The fitting parameters are given in Table 3. The value obtained for the slope $-2\mu_e^2/hc\rho^3$ allows μ_e to be determined. Taking ρ as 0.4 times the length of the molecule,[48] which is known to be 16 Å from its X-ray structure,[35] a μ_e value of 36 D is calculated. This corresponds to a unit charge separation over 7.5 Å, which is in reasonable agreement with the R_c value of 8.4 Å found in the crystal structure. It is worthwhile to compare the slope from the Lippert−Mataga analysis with that of **D[3]A**, since the ratio should reflect the ratio of R_c values.[49] By fitting the values reported in ref 40 a slope of (−25.8 ± 1.6) × 10^3 cm^{-1} and a $\nu_f(0)$ of (24.7 ± 0.3) × 10^3 cm^{-1} are obtained for **D[3]A**. The ratio of the slopes thus equals 0.53 while the ratio of the R_c values equals 0.50, which is in line with expectation. This provides strong support that in both compounds full charge separation occurs.

The high energy maxima obtained by fitting the experimental spectra of **D[3π3]A** in di-*n*-pentyl ether and di-*n*-butyl ether (Table 4) are very close to the fitted line for the ECT species (Figure 4), while the low energy maxima are on a straight line with a small slope as indicated by the dotted line in Figure 4, which is in accordance with emission from a CCT species.

If the maxima of **D[7]A**, except for the cyclohexane maximum, are fitted to eq 5, a slope of (−43.9 ± 5) × 10^3 cm^{-1} corresponding to a 37 D dipole moment or 7.7 Å charge separation is obtained. These values are all in good agreement with charge separation in an extended conformer.

Transient Absorption Spectroscopy of D[3π3π3]A, D[7π3]A, D[3π7]A, and D[11]A. Transient absorption (TA) spectra of **D[3π3π3]A**, **D[7π3]A**, and **D[11]A** were recorded upon excitation with a nanosecond (308 nm, 7 ns fwhm) XeCl excimer laser pulse in benzene. For **D[3π7]A** a 295 nm, 2.7 ns fwhm laser pulse was used. The solubility of **D[3π3π3π3]A** was too low to allow the recording of a TA spectrum. Absorption maxima and lifetimes are presented in Table 5. In

TABLE 5: Transient Absorption Maxima (nm) and Lifetimes τ (ns) of Donor−Bridge−Acceptor Compounds in Benzene at 20 °C

compound	λ_{max}	
D[3π3π3]A	340, 467	<5
D[7π3]A	340, 480	10
D[3π7]A	*a*, 470	10
D[11]A	340, 500	46

[a] Not measured.

all cases a broad band in the 460−500 nm range and a band at 340 nm were visible. The 460−500 nm band is attributed to the *N*,*N*-dialkylanilino radical cation. The *N*,*N*-dimethylaniline radical cation is known to absorb at 475 nm.[50] The 340 nm band is attributed to the dicyanovinyl radical anion.[51] It is thus concluded that for all compounds full charge separation occurs upon photoexcitation.

Steady-State Fluorescence of D[3π3π3]A, D[7π3]A, D-[3π7]A, D[11]A, D[3π3π3π3]A, [3π3]A, and [3π3π3]A. The CT fluorescence maxima and quantum yields of the longer D−B−A compounds, **[3π3]A** and **[3π3π3]A**, are given in Table 3. The fluorescence maxima and band shapes obtained for **[3π3π3]A** are virtually identical to those of **[3π3]A**, indicating that the positive charge in the charge-separated state [3π3$\pi^{\bullet+}$3]A$^{\bullet-}$ is localized on the olefinic bond adjacent to the acceptor. Apparently, Coulombic attraction between the opposite charges prevents the formation of the CT state [3$\pi^{\bullet+}$3π3]A$^{\bullet-}$.

For all D−B−A compounds the donor fluorescence is strongly reduced in intensity. For **D[3π3π3]A**, **D[7π3]A**, **D-[3π7]A**, and **D[11]A** in diisopropyl ether and more polar solvents the residual percentage of local donor emission was about 4, 6, 15, and 40%, respectively, of that of the model donor compounds. In **D[3π3π3]A**, **D[7π3]A**, and **D[3π3π3π3]A**, also the **[3$\pi^{\bullet+}$3]A$^{\bullet-}$**-like emission is strongly quenched in all solvents. Instead, for all compounds a broad structureless fluorescence band is visible. Since this band is red-shifted as compared to both the local donor fluorescence and the [3$\pi^{\bullet+}$3]-A$^{\bullet-}$-type CT fluorescence in all cases this emission stems from the fully charge-separated state, i.e., the CT state with the positive charge located on the anilino donor and the negative charge on the dicyanovinyl acceptor (see TA spectroscopy section). The quantum yield of this fluorescence is highest in cyclohexane and is strongly reduced in the more polar solvents. For compounds **D[7π3]A** and **D[3π3π3π3]A** in ethyl acetate and THF, the CT fluorescence is so low in intensity that the fluorescence spectra can be adequately described as the sum of remaining donor and [3$\pi^{\bullet+}$3]A$^{\bullet-}$-like fluorescence bands. Fluorescence spectra of **D[7π3]A** and **D[3π3π3π3]A** in other solvents could be well fitted as the sum of a donor fluorescence spectrum (either **D[3π3]** or **D[7]**), a fluorescence spectrum of **[3π3]A** or **[3π3π3]A** and a skewed Gaussian for the CT emission band originating from the fully charge-separated state (see Supporting Information for two examples). In this way it was possible to obtain proper CT fluorescence maxima and quantum yields.

When the CT fluorescence maxima are plotted against Δf, a linear relationship is found for **D[3π3π3]A**, **D[7π3]A**, **D[3π7]-A**, and **D[11]A** (Figure 5).[52] The slopes obtained for these four compounds are virtually identical and are smaller than those of **D[3π3]A**, **D[7]A**, and even **D[3]A**. When the distance between donor and acceptor R_c is estimated on the basis that the ratio of the Lippert−Mataga slopes is essentially equal to the ratio of the R_c distances (using a slope of 25.8×10^3 cm^{-1}, with R_c = 4.16 Å for **D[3]A**), extremely small values of 2.0−2.2 Å are obtained.[53] This leads to the conclusion that in all cases

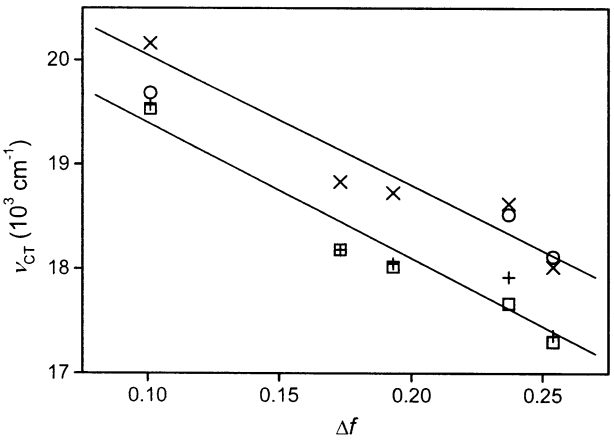

Figure 5. Plot of charge-transfer fluorescence maxima ν_f versus the solvent polarity parameter Δf: (+) **D[3π3π3]A**, (□) **D[7π3]A**, (×) **D-[3π7]A**, (○) **D[11]A**. Top line: fit for **D[7π3]A**. Bottom line: fit for **D[3π3π3]A**.

fluorescence from a folded (CCT) species is observed, in which the donor and acceptor are in close contact (see also TRMC section).

Due to its low solubility, fluorescence spectra of **D[3π3π3π3]-A** could only be obtained in three solvents. In addition to the [3$\pi^{\bullet+}$3]A$^{\bullet-}$-like emission at 415 nm, in benzene a CT emission at 577 nm belonging to a fully charge-separated state could be identified. The fact that its band maximum is almost identical to that of **D[3π3π3]A** leaves no doubt about the folded nature of the emitting species. It is conspicuous that the fluorescence maxima of **D[3π3π3]A**, **D[7π3]A**, and the single maximum obtained for **D[3π3π3π3]A** are systematically red-shifted in comparison to the maxima of **D[3π7]A** and **D[11]A** (for the latter with the exception of cyclohexane) by an average of $(7.0 \pm 0.8) \times 10^2$ cm^{-1} (0.09 ± 0.01 eV, Figure 5). In other words, the transition energy is smaller when a double bond is attached to the ring bearing the acceptor. According to eq 2 there are two possible explanations for this difference. The first is a difference in reduction potential of the acceptor. However, cyclic voltammetry revealed that the onsets of the irreversible reduction waves of **[3π3]A** and **[7]A** do not differ by more than 0.02 V, which means that the reduction potentials are equal within experimental error. The second possibility is a difference in reorganization energy λ_i' upon charge recombination in the folded state. Apparently, the nature of the bond connecting the ring bearing the acceptor to the other part of the molecule is of interest for the reorganization energy of the CCT species, whereas the bond type near the donor site does not have an effect (see below).

Time-Resolved CT Fluorescence. Charge-transfer fluorescence decay times τ_f for all D−B−A compounds in a few solvents are given in Table 6. Lifetimes were measured with a streak camera system upon 295 nm excitation (fwhm 2.7 ns). To obtain a better time-resolution, in benzene and cyclohexane additional SPC measurements were performed (excitation 312−315 nm, fwhm instrument response time ~17 ps).

In steady-state measurements on **D[3π3]A**, two fluorescence bands were observed in cyclohexane and benzene (see "Solvent Dependence of the Steady-State Fluorescence of **D[3π3]A** and **D[7]A**" section) of which one was assigned to an ECT species and the other to a CCT species. It was noted previously[18] that the CCT fluorescence of **D[3π3]A** in cyclohexane seems to appear instantaneously upon excitation. This was tentatively attributed to the occurrence of charge separation in a partly folded conformation or to very rapid folding of a stretched

TABLE 6: Charge-Transfer Fluorescence Rise Times τ_i and Decay Times τ_f (in ns) of Donor−Bridge−Acceptor Compounds in Various Solvents at 20 °C. Data Determined near the Maximum of the Fluorescence Band (See Table 3)

	D[3π3]A		**D[7]A**		**D[3π3π3]A**		**D[7π3]A**		**D[3π7]A**		**D[11]A**	
solvent	τ_i	τ_f	τ_i	τ_f	τ_i	τ_f	τ_i	τ_f	τ_i	τ_f	τ_i	τ_f
cyclohexane	*a*	0.24 (ECT); 12.6 (20[b])	1.3	13 (24[b])	*a*	20.5	1.4	13.6	0.9	22.9	*c*	21
di-*n*-pentyl ether												20
benzene	*a*	0.36 (ECT); 1.6 (2[b])	*a*	19 (36[b])	0.21	2.7	0.8	4.3	0.7	10.9	*a*	31
di-*n*-butyl ether				29						6.4		19
diisopropyl ether		∼1.6		14		2.7		4.0		10.5		19

[a] Rise of the fluorescence signal not observed. [b] Values from ref 18. [c] Not observed as a consequence of too low intensity.

TABLE 7: Fluorescence Lifetimes (in ns) [Quantum Yields][18] of Donor and Acceptor Chromophores at 20 °C

solvent	**D[3π3]**	**D[7]**	**[3π3]A**	**[3π3π3]A**
cyclohexane	1.87 [0.25]	1.82 [0.25]		
benzene	2.66 [0.34]	2.56 [0.35]	1.32	1.50
THF	2.50	2.43	2.07	2.31

conformation. We have now determined the lifetime of the ECT state to be 0.24 ns in cyclohexane and 0.36 ns in benzene and confirmed the instantaneous appearance of CCT fluorescence. This means that the decay of the ECT fluorescence is *not* coupled to the appearance of the CCT fluorescence. This observation shows that different conformers of the fully charge-separated state are present directly after photoexcitation followed by charge separation. The ECT species, for instance, could be the anti conformer while the already partly folded syn conformer could be held responsible for the apparent instant appearance of CCT fluorescence.

In cyclohexane the lifetimes of the CCT species of the D−B−A compounds are in the range 13−23 ns. Upon increasing the solvent polarity, the CCT lifetimes of **D[3π3]A**, **D[3π3π3]A**, and **D[7π3]A** decrease dramatically, while for **D-[7]A** and **D[11]A**, containing fully saturated bridges, this is not the case. For example, in benzene, which is considered to be a quasi polar solvent (as invoked from CT emission maxima), the lifetime of the CCT state of **D[3π3π3]A** is approximately 10 times shorter than that of **D[11]A**. For **D[3π7]A** intermediate behavior is observed. By comparing the CCT lifetimes of **D-[3π3π3]A** and **D[7π3]A** it appears that the extra olefinic bond next to the donor in **D[3π3π3]A** has only a very small accelerating effect on the recombination rate (factor of about 1.5). These observations indicate that the olefinic bond provides an additional decay channel and that this channel becomes less important as the distance between the olefinic bond and the acceptor is enlarged. This is quite remarkable since the compounds are in a folded conformation. The most probable decay channel is governed by an increased coupling of the CCT state with the $[3\pi^{\bullet+}3]A^{\bullet-}$-like "local" CT state. This state has a short lifetime (see Table 7) in all solvents employed and its energy drops faster with increasing solvent polarity than that of the CCT states (see the slopes of Lippert−Mataga plots in Table 3).[54] Thus, the energetic distance between the $[3\pi^{\bullet+}3]A^{\bullet-}$ state and the CCT state decreases upon increasing solvent polarity by which the coupling between these states is enlarged. A small degree of admixture of a short-lived state can strongly reduce the lifetime of a CT state.[55] If the degree of mixing is small, the magnitude of the CT state's dipole moment is not substantially affected. For **D[3π7]A** it is anticipated that the $D[3\pi^{\bullet+}7]A^{\bullet-}$ state lies higher in energy than the $D[3\pi3\pi^{\bullet+}3]A^{\bullet-}$ state of **D[3π3π3]A** due to the larger distance between the charges. This state could provide the additional decay channel in **D[3π7]A**.

Unexpectedly fast charge recombination possibly due to an intermediate $D_2-D_1^{\bullet+}-A^{\bullet-}$ state has been observed before[56] for a trichromophoric compound consisting of a 1,3-diphenylpropanedioate boron oxalate acceptor, a 4,4′-biphenylene D_1 donor and a methoxynaphthalene D_2 donor. A 3- to 4-fold increase in the charge-recombination rate upon addition of two methoxy groups to a benzene spacer in a trichromophoric compound with a zinc porphyrin donor and a 1,4-naphthoquinone acceptor has been observed by Wasielewski et al.[57] In this case a virtual $D_2-D_1^{\bullet+}-A^{\bullet-}$ state was held responsible for the increased charge-recombination rate.

TABLE 8: TRMC Data for Donor−Bridge−Acceptor Compounds

compound	τ (ns)	μ^2/θ[a] (D^2 ps^{-1})	μ_{cyl} (D)	μ_{sph} (D)
D[3π3]A[18]	2.0	3.43	27.9	16.8
D[7]A[18]	36.0	3.74	29.4	17.6
D[3π3π3]A	2.2	2.63	32.3	16.4
D[7π3]A	5.0	2.50	31.6	15.7
D[3π7]A	6.5	4.73	43.6	21.8
D[11]A	25	5.17	45.5	22.8
D[3π3π3π3]A	2.2	2.63	40.7	18.2

[a] Values are corrected for the quantum yield for charge separation as obtained from time-resolved fluorescence measurements (Table 9).

Time-Resolved Microwave Conductivity (TRMC). Using the TRMC technique, the change in microwave conductivity $\Delta\sigma$ occurring on flash-photolysis at 308 nm of benzene solutions of the present compounds was measured. To a good approximation $\Delta\sigma$ is related to the concentration of excited states formed N_e, the excited-state dipole moment μ_e, and the dipole relaxation time θ via[58,59]

$$\Delta\sigma = \frac{(n^2+2)^2 N_e}{27 k_B T} \cdot \frac{\mu_e^2}{\theta} \qquad (7)$$

From convolution fits to the TRMC transients, the excited-state lifetime τ_e and the parameter μ_e^2/θ can be derived, and these are given in Table 8. In deriving μ_e^2/θ, the fact that the quantum yields of formation of the dipolar excited states of the longer-bridge compounds are somewhat smaller than unity as derived from the optical data, was taken into account (Table 9).

The TRMC results confirm the highly dipolar, charge-transfer nature of the relaxed S_1 states of all of the D−B−A compounds investigated. The decay times of the TRMC transients are in reasonable agreement with the decay times found for the transient absorption and the fluorescence of the same compounds in benzene (Tables 5 and 6). Of particular interest is the influence of the bridging unit on the decay time since this is governed by charge recombination involving electron transfer between the donor and acceptor moieties.

For **D[7]A** and **D[3π3]A**, both of which have seven carbon−carbon bonds between donor and acceptor and close to equal donor−acceptor distances in the ground state, the recombination time is more than an order of magnitude shorter for the latter

TABLE 9: Donor Fluorescence Lifetimes (τ in ns) and Rates of Photoinduced Intramolecular ET (k_{et} in s^{-1} [Calculated Quantum Yield of Charge Separation Φ_{et}]) of Donor−Bridge−Acceptor Compounds at 20 °C

	D[3π3π3]A		**D[7π3]A**		**D[3π7]A**		**D[11]A**		**D[3π3π3π3]A**	
solvent	τ	$k_{et}/10^9$	τ	$k_{et}/10^9$	τ	$k_{et}/10^9$	τ	$k_{et}/10^9$	τ	$k_{et}/10^9$
cyclohexane	0.17	5.3 [0.91]	0.30	2.8 [0.84]	0.20	4.5 [0.89]	0.46	1.6 [0.75]	*a*	*a*
benzene	0.11	8.7 [0.96]	0.21	4.4 [0.92]	0.18	5.2 [0.93]	0.59	1.3 [0.77]	0.93, 1.5	0.70 [0.65]
THF	0.19	4.9 [0.92]	0.36	2.4 [0.85]	0.38	2.2 [0.85]	0.92	0.68 [0.62]	1.06, 1.92	0.54 [0.58]

[a] Solubility too low.

compound. The presence of a central π-bond in the bridge would therefore appear to have a marked accelerating effect on electron transfer.

For the four compounds with a total of 11 carbon−carbon bonds in the bridge, **D[11]A**, **D[3π7]A**, **D[7π3]A**, and **D[3π3π3]-A**, the lifetime toward recombination is found to decrease by a factor of approximately 5 in going from the completely saturated bridge to bridges containing one π-bond. A further decrease in lifetime by a factor of 2−3 is found on introducing a second π-bond in the bridge. The present results on both the seven- and 11-bond D−B−A compounds therefore clearly demonstrate the pronounced positive influence on charge recombination of the substitution of a π- for a σ-bond in the bridging unit. While we cannot exclude the possibility that the effects observed arise to a certain extent from the greater conformational flexibility of the bridges containing double bonds, we consider that this is insufficient to explain the results completely. We conclude that the intervening double bonds have a super-exchange function and facilitate charge recombination via electron transfer through the bridge.

As discussed in previous sections, there is evidence that the geometrical conformation of the molecules in the excited state may differ considerably from that in the ground state. Because of this it is not possible to make a reasonable estimate of the rotational relaxation time θ, which is required to derive an estimate of the dipole moment of the relaxed S_1 state from the values of μ^2/θ determined experimentally. In Table 8 we therefore give two estimates for μ_e, one of which, μ_{cyl}, is based on a value of θ estimated for an outstretched, cylindrical geometry, and the other, μ_{sph}, is based on a compact spherical geometry.[59]

The value of μ_{sph} corresponds to the smallest dipole moment possible for S_1. For all D−B−A compounds this is significantly larger than the value of 10 to 12 D associated with close-contact, donor−acceptor exciplexes. On the other hand the values of μ_{cyl} are in general smaller than would be expected for complete charge separation between donor and acceptor moieties in the ground-state geometry, i.e., ca. 40 and 60 D for the seven- and 11-bond bridged compounds, respectively. The TRMC results are therefore in general agreement with the previous conclusions that a substantial change in the molecular geometry occurs after charge separation which results in a decrease in the distance between the donor and acceptor moieties. Complete folding of the bridge, resulting in the formation of a contact donor−acceptor pair does not however occur for any of the compounds studied.

It is conspicuous that the μ_e^2/θ data divide the four 11-bonds-bridged compounds into two pairs. The values for the compounds with an olefinic bond next to the acceptor are much smaller than those for the compounds with a single bond at the corresponding position. This could well be related to the occurrence of different structures of the two sets of compounds (which affects θ rather than μ_e, since the Lippert−Mataga slopes are similar). This is supported by the red-shifted fluorescence maxima of **D[3π3π3]A** and **D[7π3]A** as compared to those of **D[3π7]A** and **D[11]A** which indicate that their CCT state is stabilized.

Energetics of Charge Separation. An important quantity in the analysis of the charge-separation process is the Gibbs energy difference ΔG between the initial and final states of the charge-separation step $D^{\bullet+}-B-A^{\bullet-} \leftarrow D^*-B-A$. A well-known way to estimate ΔG is by means of the Weller equation.[60,61] The usefulness of the Weller equation critically depends on the choice of the mean ion radius r and the donor acceptor distance R_c. A more direct way to obtain an estimate for ΔG is possible when both charge-transfer absorption and emission bands can be measured. The energy of a CT state can then be estimated by the mean value of the absorption and emission maxima.[42] For most of the D−B−A compounds in the present study these values cannot be obtained, either because CT absorptions involving full charge separation are not discernible in the spectra or because of overlap with other bands. For **D[3π3]A** in cyclohexane, however, the onset of a CT absorption band and the emission from an ECT species in cyclohexane could be determined. Although a maximum of the CT absorption band is not present, the intersection of the onsets of both bands also yields E_{00}. Thus, using the spectra represented in a reduced form[62] and scaled in intensity in such a way that the mirror image relationship holds for the onsets of both bands, the E_{00} value for the CT transition in cyclohexane is estimated as 3.52 eV. For **D[7]** the E_{00} value obtained in this way in cyclohexane is 3.92 eV, so that $\Delta G \sim -0.40$ eV for charge separation in **D[3π3]A** in cyclohexane. This value is in reasonable agreement with our previous[18] estimate of −0.52 eV which was obtained by using the Weller equation. For the shorter homologue **D[3]A** using the CT absorption and fluorescence maxima $h\nu_a = 3.63$ eV (342 nm) and $h\nu_f = 2.77$ eV (22.3×10^3 cm^{-1}) in *n*-hexane[40] a value for ΔG of ~ -0.72 eV is calculated. When obtained in a nonpolar solvent for which the outer or solvent reorganization energy can be neglected,[63] CT absorption and fluorescence maxima also give access to the inner reorganization term λ_i via[2]

$$h\nu_a - h\nu_f = 2\lambda_i \qquad (8)$$

Upon use of the same data, for **D[3]A** a value for λ_i of approximately 0.4 eV is obtained. This value is expected not to depend much on the donor−acceptor separation distance R_c, since the main structural reorganization upon charge transfer takes place on the donor and acceptor sites. Thus, assuming that $\lambda_i \simeq 0.4$ is also valid for **D[3π3]A** and **D[7]A**, it can be concluded that for these compounds (in cyclohexane) charge transfer takes place near the optimal region where $-\Delta G = \lambda$. For the longer homologues ET in cyclohexane will almost certainly take place in the normal region for which $-\Delta G < \lambda$ since the longer donor−acceptor distance R_c for these compounds will decrease the driving force for charge separation. It is known that with increasing medium polarity, both the driving force and the total reorganization energy λ increase, but since these contributions tend to cancel each other[2] it is expected that

the above conclusions will hold throughout the applied solvent polarity range.

Bridge Dependence of the Charge-Separation Process. To compare the charge-separation dynamics as a function of bridge topology, we determined the fluorescence lifetimes of the model donors and acceptors (Table 7). The emission could in all cases be fitted well with a single exponential. In addition, the decay of the residual local donor emission of the D−B−A compounds was measured (Table 9). For **D[3*π*3]A** and **D[7]A** no reliable decay data could be obtained. In the case of compounds **D-[3*π*3*π*3]A**, **D[7*π*3]A**, **D[3*π*7]A**, and **D[11]A**, the residual local donor fluorescence could be satisfactorily fitted with two lifetimes: a very short component and a component with a lifetime in the order of those of the model donor compounds **D[3*π*3]** and **D[7]**. For **D[3*π*3*π*3*π*3]A** more exponentials were necessary. The component comparable to the lifetime of the model donor compounds probably stems from minute amounts of molecules which lack the acceptor. When it is assumed that the short component of the donor fluorescence decay is shortened only by the additional pathway of ET and that the latter process is irreversible, rates of intramolecular electron transfer k_{et} can be calculated with

$$k_{et} = \frac{1}{\tau_f(\mathrm{DBA})} - \frac{1}{\tau_f(\mathrm{D})} \tag{9}$$

where τ_f(DBA) is the donor fluorescence lifetime in the D−B−A compound and τ_f(D) the fluorescence lifetime of the appropriate model donor compound (**D[3*π*3]** or **D[7]**). Within the same approximation the quantum yield of ET Φ_{et} can be calculated with

$$\Phi_{et} = \frac{k_{et}}{k_f(\mathrm{D}) + k_{nr}(\mathrm{D}) + k_{et}} = \frac{k_{et}}{1/\tau_f(\mathrm{D}) + k_{et}} = \frac{\tau_f(\mathrm{D}) - \tau_f(\mathrm{DBA})}{\tau_f(\mathrm{D})} \tag{10}$$

where k_f(D) and k_{nr}(D) are the fluorescent and nonradiative decay rates of the model donor compound, respectively. Obtained values of k_{et} and Φ_{et} are also collected in Table 9.

With the SPC setup the rise of the CT fluorescence of **D-[3*π*3*π*3]A**, **D[7*π*3]A**, and **D[3*π*7]A** in cyclohexane and benzene was observed, with time constants in the range 0.2−1.4 ns. Unfortunately, the CT fluorescence band of **D[11]A** was very weak which, in combination with its low solubility, hampered a reliable study of the possible rise of CT fluorescence. When the lifetimes of donor fluorescence of **D[3*π*3*π*3]A**, **D[3*π*7]A**, **D[7*π*3]A**, and **D[11]A** are compared to the time constants for the ingrowth of the CCT fluorescence (Table 6) it can be seen that in all cases where both values are available the former are substantially shorter. In other words, the decay of the local donor fluorescence does not reflect the formation of the CCT state. An intermediate state has to be present and this is supposed to be an ECT state. Hence, ET in an extended conformer occurs which is followed by folding to a compact or CCT state. This sequence is known as "harpooning".[20−23] For **D[7]A** a harpooning mechanism is operative as well, but in the case of **D[3*π*3]-A** ingrowth of the CCT emission could not be detected whereas decay of the ECT emission was observed (see above). This can be explained by assuming different behavior for the syn and anti conformers of **D[3*π*3]A**. ECT emission may only be produced by the anti conformer whereas the rapid appearance of CCT emission may originate from contraction of syn conformers. The latter are already partly folded in the ground state.

In the following analysis a survey of the influence of bridge topology on the rate of ET k_{et} is made. Although formally incorrect, it will be assumed that the ET rate processes of the different conformers can be represented by a single rate constant. For **D[3*π*3*π*3]A**, **D[3*π*7]A**, **D[7*π*3]A**, and **D[11]A** the electron transfer was found to occur in an extended conformation prior to folding. In that case the electronic coupling energy between reactant and product states H_{rp} is expected to be small so that the ET process is nonadiabatic and can be described by semiclassical electron transfer theory.[64] The rate constant k_{et} is then given by[63]

$$k_{et} = \frac{4\pi^2}{h} H_{rp}{}^2 \mathrm{FCWD} \tag{11}$$

where FCWD is the Franck−Condon weighted density of states. If it is also assumed that compounds of comparable length and identical donor−acceptor pair such as used here possess a similar FCWD value, differences in k_{et} will directly reflect differences in $H_{rp}{}^2$. Since H_{rp} is predominantly determined by the nature of the bridge, k_{et} also directly gives the effect of incorporation of an olefinic bond in the bridge.

The following trend is observed: the rates for **D[3*π*3*π*3]A** are roughly 2 times faster than those for **D[7*π*3]A** and **D[3*π*7]-A**, which are of similar magnitude. The rates for **D[7*π*3]A** and **D[3*π*7]A** in turn are about 3 times faster than those for **D[11]-A**. For the quantum yield of charge separation also the trend **D[3*π*3*π*3]A** > **D[7*π*3]A** ∼ **D[3*π*7]A** > **D[11]A** is found. Although this suggests that replacement of the first single bond by a double bond has a larger effect than replacement of the second, on average an increase in the rate of charge separation of 3.0 ± 0.8 per olefinic bond is observed. This corresponds to an increase of the electronic coupling of 1.7 ± 0.2 per bond. At this point it is of interest to note that the introduction of a double bond increases the electronic coupling in two hardly separable ways. It increases the donor−acceptor interaction since the bridge facilitates transport of electronic effects. Concurrently, the donor−acceptor distance is reduced, as a C═C double bond is shorter than a C−C single bond. The shorter distance is expected to affect ΔG, λ and FCWD, which is a function of both ΔG and λ. As it is likely that k_{et} follows the usual distance dependence $k_{et} \propto \exp(-\beta R_c)$, the net effect will be that upon going from **D[11]A** to **D[3*π*3*π*3]A** k_{et} also increases as a consequence of the shorter donor−acceptor distance. This makes the factor of 1.7 ± 0.2 an upper limit to the purely electronic coupling. When viewed in terms of the number of bonds, one may however also state that the effect on the electronic coupling is a factor of 1.7 ± 0.2 per double bond.

An effect of the incorporation of two olefinic bonds on the rate of charge separation has been observed by de Rege et al.[65] as well. They found that incorporation of two double bonds in a saturated bicyclic hydrocarbon bridge enhances the rate of charge separation by a factor of 2. Introduction of exocyclic double bonds in the oligo(cyclohexyl) bridge thus has a larger effect. This larger effect might find its origin in the favorable interaction between the double bond and H_{ax}−C−C−H_{ax} units.[12,13]

Solvent Dependence of the Rate of Charge Transfer in D[11]A. To obtain an indication of the magnitude of the barrier for ET in **D[11]A** (for which the donor−acceptor separation distance is considered to be well-defined) the donor fluorescence lifetimes of this compound and those of **D[7]** were measured in six solvents (Table 10). ET rates obtained from these data via eq 9 range from 0.68×10^9 s^{-1} in THF to 1.6×10^9 s^{-1} in cyclohexane. Hence, the effect of the medium polarity on k_{et} is

TABLE 10: Donor Fluorescence Lifetimes (τ in ns) of D[7] and D[11]A and Rates of Photoinduced Intramolecular ET [k_{et} in s^{-1} [Calculated Quantum Yield of Charge Separation Φ_{et}]] for D[11]A in Various Solvents at 20 °C

	D[7]	D[11]A	
solvent	τ	τ	$k_{et}/10^9$
cyclohexane	1.82	0.46, 1.6	1.6 [0.75]
di-*n*-pentyl ether	2.1	0.73, 2.2	0.89 [0.65]
di-*n*-butyl ether	2.10	0.84, 2.0	0.71 [0.60]
diisopropyl ether	1.99	0.75, 1.8	0.83 [0.62]
THF	2.43	0.92, 1.9	0.68 [0.62]
benzene	2.56	0.59, 2.7	1.3 [0.77]

very moderate. This indicates that in **D[11]A** the donor−acceptor distance is such that the barrier for ET is of similar magnitude in all solvents. According to design criteria for ET systems,[66] this near solvent independence suggests that the donor−acceptor combination, along with the bridge, provides an efficient ET system. This boils down to the fact that the quantity $E_{ox}(\mathbf{D}) - E_{red}(\mathbf{A}) - E_{00}$ will not deviate more from the optimal value than ca. 0.5 eV. A glance at Table 9 indicates that this is valid for the whole series of compounds **D[3π3π3]A**, **D[7π3]A**, **D[3π7]A**, and **D[11]A**. Note that for **D[3π3]A** and **D[7]A** it was inferred that ET will be close to barrierless, since it was found that $-\Delta G \sim \lambda$.

Conclusions

Photoinduced ET takes place in extended conformers of **D[7]A**, **D[3π3π3]A**, **D[7π3]A**, **D[3π7]A**, **D[11]A**, and **D[3π3π3π3]A** producing a fully charge-separated state. The ET step is followed by folding, even in solvents as polar as diethyl ether. For **D[3π3]A** both the extended and folded fully charge-separated CT conformers were detected, but the decay of the ECT fluorescence is not coupled to the ingrowth of the CCT fluorescence. This is explained by the presence of both syn and anti conformers in solution, which exhibit markedly different excited-state behavior.

The presence of an olefinic bond in the bridge influences the charge-separation and -recombination rates, as well as the excited-state properties of the studied D−B−A compounds considerably. The fluorescence maxima of CCT states with a [3π3]A-type acceptor are consistently 0.09 eV red-shifted as compared to those of compounds with a [7]A-type acceptor. This might be explained by a structural difference in the two sets of CCT conformers. TRMC measurements also point to a structural difference in the CCT species.

In the series **D[3π3π3]A**, **D[3π7]A**, **D[7π3]A**, and **D[11]A**, the rate of charge separation $D^{\bullet+}-B-A^{\bullet-} \leftarrow D^{*}-B-A$ increases with a factor of 3.0 ± 0.8 per olefinic bond and is not strongly affected by the position of the olefinic bond in the bridge. Since the incorporation of an olefinic bond also slightly reduces the donor−acceptor distance, this corresponds to a maximum factor of 1.7 ± 0.2 for the increase of the electronic coupling with the introduction of an olefinic bond. The charge-recombination rate of the CCT state increases with increasing solvent polarity for compounds whose bridge contains an olefinic bond. This behavior is explained by a recombination process that involves $D-B^{\bullet+}-A^{\bullet-}$ states. The effect is most pronounced in case the olefinic bond is located next to the acceptor, i.e., for compounds with a [3π3]A-like acceptor. Thus, in benzene the recombination rate for **D[3π3π3]A** is 11 times that found for **D[11]A**. Hence, although incorporation of a double bond accelerates the charge-separation process, the effect on the charge-recombination rate is even more pronounced.

Experimental Section

General. All reactions and distillations were carried out under an atmosphere of dry N_2 unless stated otherwise. Commercially available reagents were used without further purification. THF and diethyl ether were distilled from Na/benzophenone prior to use. MeCN was distilled from CaH_2. EtOH was stored on molecular sieves (3 Å). *N*,*N*,*N*′,*N*′-Tetramethylethylenediamine (TMEDA) was dried by boiling with $LiAlH_4$ under reflux for 3 h, followed by distillation under reduced pressure (0.01 Torr).[67] Column chromatography was performed using ACROS silicagel 0.035−0.070 mm, pore diameter ca. 6 nm. Thin-layer chromatography was performed on Merck silicagel 60 F_{254}. Spots were detected by the use of iodine vapor and/or UV light. Melting points were determined on a homemade melting point apparatus or on a Mettler FP5/FP51 photoelectric melting point apparatus and are uncorrected. Gas chromatography was performed on a Varian 3350 instrument equipped with a DB-5 (i.d. 0.309 mm, 25 m) capillary liquid-phase column and an FID using N_2 as carrier gas. NMR spectra were recorded on a Bruker AC 300 spectrometer operating at 300.13 MHz for ^{1}H NMR and at 75.47 MHz for ^{13}C NMR. Samples were dissolved in deuterated chloroform unless stated otherwise. Chemical shifts (in ppm) are given relative to internal TMS (0 ppm) in the case of ^{1}H NMR and relative to $CDCl_3$ (77.00 ppm) in the case of ^{13}C NMR. Infrared spectra were recorded on a Mattson Galaxy Series FTIR 5000 operating with 2 cm^{-1} resolution. Solids were measured in KBr pellets, while liquid materials were measured as a thin film between NaCl plates. Peak maxima are given in cm^{-1}, while intensities are designated as s (strong), m (medium), or w (weak). Molecular mechanics (MM2) calculations were performed using the MM2 force field as implemented in CambridgeSoft Chem3D Pro, version 4.0 (1997). Cyclic voltammetry was performed with a EG&G Princeton Applied Research model 263A potentiostat/galvanostat. The scan rate employed was 50 mV s^{-1}. Measurements were conducted in MeCN (freshly distilled from CaH_2) using anhydrous tetrabutylammonium hexafluorophosphate in 0.1 M concentration as the electrolyte. The solution was purged with N_2 prior to the measurement. A three-electrode setup was used, with a Pt disk electrode (area 0.78 mm^2), a Pt counter electrode and a Ag/$AgNO_3$ (0.1 M in MeCN) reference electrode. Solute concentrations were 2 mM. MALDI TOF-MS (positive-ion mode) was performed on a Perkin-Elmer/PerSeptive Biosystems Voyager-DE-RP MALDI TOFF-MS [N_2 laser; λ_{exc} = 337 nm (3 ns pulses)]. TOF-MS spectra were recorded in the reflectron mode. The samples **D[3π3π3π3]A** and **D[3π7]A** were mixed with dihydroxybenzoic acid solution (3 mg mL^{-1}); 1 μL of the suspension was loaded on the Au-sample plate.

Steady-State Absorption and Fluorescence Spectroscopy. Details of the instrumentation used to record absorption and fluorescence spectra are given in ref 34. Fluorescence quantum yields were determined relative to quinine sulfate in 0.5 M H_2SO_4 (ϕ = 0.546)[68] at 20 °C (excitation at 300 nm). To accurately measure the low (ϕ < 0.05) quantum yields of CT emission a solution of quinine sulfate with known absorbance at the excitation wavelength was diluted by a known factor in such a way that the maximum emission intensity of the quinine sulfate solution was comparable to that of the sample. To correct for the wavelength dependence of the fluorescence intensity due to the use of monochromators, the fluorescence intensity $I(\lambda)$ was multiplied by λ^2 when converting the spectra to an energy scale. Solutions were purged with Ar for at least 10 min prior to measurement. Corrections for solvent refractive indices were made according to Eaton[68] when needed.

Spectroscopic grade solvents were used throughout with the following exceptions; diisopropyl ether (ACROS 99+ %) and di-*n*-butyl ether (Fluka, p.a.; low in aromatic compounds; ≥99.5%) were stirred with $LiAlH_4$ for at least 1 day and then distilled. Di-*n*-pentyl ether (Fluka, 99%) was purified as follows. Five parts of the ether were stirred with one part of sulfuric acid (Merck, p.a. 95−97%) for 1 day. The brown mixture was poured into 2.5 parts of water and the layers were separated. The organic layer was washed with water, saturated $NaHCO_3$ solution and water (similar volumes), dried on $MgSO_4$, and filtered. This procedure was repeated until a brown color did not develop anymore upon stirring with sulfuric acid. Subsequently, the ether was treated as described for diisopropyl ether. Ethyl acetate (ACROS, HPLC grade, ≥99.5%) was stirred with CaH_2 for 3 days and subsequently distilled. THF and diethyl ether were distilled from Na/benzophenone. All purified solvents were checked for spurious emission.

Time-Resolved Measurements. Picosecond single-photon-counting (SPC) fluorescence decay traces were measured and analyzed using the setup and computer programs described in ref 69. Samples were degassed by purging with Ar for 10 to 15 min and were excited at 310−320 nm. Time-resolved microwave conductivity was performed as described in ref 18. Transient absorption spectroscopy of **D[3*π*3*π*3]A**, **D[7*π*3]A**, and **D[11]A** was performed using the equipment and procedures described in ref 18. In the case of **D[3*π*7]A** the equipment and procedures described in ref 34 were used.

Synthesis. The syntheses of **D[3*π*3]A**, **D[7]A**, **D[3*π*3]**, **D-[7]**, and **[3*π*3]A** have been described in ref 18. The syntheses of **[3*π*3]A** and **[3*π*7]A** have been described in ref 70. **D[3*π*3]A** was exhaustively purified by column chromatography with CH_2Cl_2 as eluent followed by two crystallizations from ethyl acetate (6.5 mg mL^{-1}, reflux until reaching room temperature) under a N_2 atmosphere. The purity was monitored by recording the emission spectrum in THF, the relative intensity of "local" emission functioning as an indicator for the amount of impurity. **D[7]A** was purified by column chromatography with CH_2Cl_2 as eluent. The synthetic procedures for the preparation of **2e** and D−B−A compounds **D[3*π*3*π*3*π*3]A**, **D[7*π*3]A**, **D[11]A**, and **D[3*π*7]A** are available as Supporting Information.

Synthesis of D−B−A Compounds. 9-[1-Hydroxy-4-(1-phenylpiperidin-4-ylidene)cyclohexyl]-3,3-dimethyl-1,5-dioxaspiro[5.5]undecane-9-carboxylic acid (3). A two-necked flask was filled with THF (50 mL) and diisopropylamine (2.17 g, 21.7 mmol). To this solution *n*-butyllithium in *n*-hexane (14.5 mL of a 1.46 M solution, 21.2 mmol) was added at −40 °C. After the mixture was stirred for 30 min, 3,3-dimethyl-1,5-dioxaspiro[5.5]undecane-9-carboxylic acid (**2e**)[11] (2.37 g, 10.4 mmol) in THF (50 mL) was added at −40 °C. The reaction mixture was stirred at 50 °C for two h and recooled to −40 °C. The compound 1-phenylpiperidin-4-one (**19**)[40] (2.63 g, 10.3 mmol) in THF (50 mL) was added, and the reaction mixture was stirred at 50 °C for another 2 h. After the mixture was cooled to room temperature, the resulting suspension was poured on ice (150 g) and diluted with diethyl ether (200 mL). The layers were separated, and the water layer was washed with diethyl ether (2 × 100 mL). A white precipitate formed in the water layer which was filtered off and dried in vacuo over KOH. The white solid (lithium salt of **3**) was then suspended in water (50 mL) and acidified to pH 1 using 3 M HCl solution. The suspension was stirred for 90 min, and the white solid was filtered off and dried in vacuo over KOH, yielding **3** (2.35 g, 47%): mp 210 °C (dec). FT-IR $\tilde{\nu}_{max}$: 3434, 2971, 2955, 2911, 2843, 2900−2300, 1672, 1493, 1462, 1438, 1119, 770, 700.

4-[4-(3,3-Dimethyl-1,5-dioxaspiro[5.5]undecan-9-ylidene)-cyclohexylidene]-1-phenylpiperidine (4). To a suspension of *β*-hydroxy acid **3** (2.35 g, 4.86 mmol) in MeCN (50 mL) was added *N*,*N*-dimethylformamide dineopentyl acetal (2.35 g, 10.2 mmol) and after stirring for 1 h at room temperature the reaction mixture was heated to reflux overnight. The resulting yellow solution was cooled to −20 °C and the resulting precipitate was filtered off, washed with cold MeCN, and dried to yield an off-white solid (1.73 g, 85%): mp 222 °C (dec). ^{1}H NMR *δ*: 0.98 (s, 6H), 1.79−1.83 (m, 4H), 2.23−2.30 (m, 12H), 2.44−2.48 (m, 4H), 3.20−3.24 (m, 4H), 3.53 (s, 4H), 6.78−6.82 (m, 1H), 6.91−6.93 (m, 2H), 7.22−7.25 (m, 2H). ^{13}C NMR *δ*: 22.8, 25.1, 29.0, 29.4 (2 ×), 30.2, 33.4, 50.4, 70.1, 97.8, 115.9, 118.8, 125.6, 128.2, 129.0 (2 ×), 130.1, 151.4. FT-IR $\tilde{\nu}_{max}$: 3096, 3067, 3040, 3023, 2976, 2953, 2928, 2890, 2866, 2839, 2830, 1599, 1462, 1445, 1429, 1113, 1099, 748, 685.

4′-(1-Phenylpiperidin-4-ylidene)-1,1′-bi(cyclohexyliden)-4-one (5). Acetal **4** (1.72 g, 4.09 mmol) was dissolved in THF (250 mL), and 5% HCl solution (25 mL) was added. The mixture was heated to reflux for 4 h. After cooling to room-temperature THF was removed under reduced pressure and the resulting suspension was extracted with $CHCl_3$ (2 × 150 mL). The combined organic extracts were washed with a saturated $NaHCO_3$ solution and water. Drying over $MgSO_4$, followed by evaporation of the solvent under reduced pressure, gave an off-white solid (1.25 g, 91%): mp 155 °C (dec). ^{1}H NMR *δ*: 2.32 (s, 8H), 2.39−2.44 (m, 4H), 2.45−2.49 (m, 4H), 2.55−2.59 (m, 4H), 3.21−3.25 (m, 4H), 6.79−6.84 (m, 1H), 6.91−6.94 (m, 2H), 7.23−7.28 (m, 2H). ^{13}C NMR *δ*: 26.5, 28.8, 28.9, 29.3, 40.5, 50.4, 115.9, 118.9, 124.3, 126.1, 129.0, 129.4, 131.9, 151.3, 212.9. FT-IR $\tilde{\nu}_{max}$: 3092, 3063, 3040, 3017, 2971, 2959, 2890, 2841, 2828, 2810, 1723, 1599, 1460, 1438, 1423, 758, 696.

[4′-(1-Phenylpiperidin-4-ylidene)-1,1′-bi(cyclohexyliden)-4-ylidene]malononitrile (D[3*π*3*π*3]A). A mixture of ketone **5** (0.63 g, 1.88 mmol), malononitrile (0.24 g, 3.64 mmol), ammonium acetate (0.19 g, 2.5 mmol) and acetic acid (0.45 mL, 7.9 mmol) in benzene (130 mL) was refluxed for 2 h in a Dean−Stark apparatus. After ca. 100 mL of benzene-water mixture was distilled off, the remaining suspension was cooled to room temperature. The greenish precipitate formed was filtered off, washed with benzene and purified by column chromatography (silica; eluent $CHCl_3$). This gave **D[3*π*3*π*3]A** (0.41 g, 57%) as a greenish solid: mp 214 °C. ^{1}H NMR *δ*: 2.30 (s, 8H), 2.46−2.50 (m, 8H), 2.73−2.77 (m, 4H), 3.21−3.24 (m, 4H), 6.79−6.84 (m, 1H), 6.91−6.94 (m, 2H), 7.23−7.26 (m, 2H). ^{13}C NMR *δ*: 28.2, 28.8, 29.0, 29.4, 34.5, 50.4, 83.0, 111.6, 115.9, 118.9, 123.4, 126.5, 129.0, 129.1, 133.2, 151.3, 184.9. FT-IR $\tilde{\nu}_{max}$: 3090, 3077, 2982, 2969, 2903, 2839, 2230, 1599, 1504, 1465, 1439, 1425, 750, 688. Anal. Calcd for $C_{26}H_{29}N_3$: C, 81.42; H, 7.62; N, 10.96. Found: C, 81.21; H, 7.70; N, 10.90.

Acknowledgment. This research has been financially supported (W. D. O.) by the Council for Chemical Sciences of The Netherlands Organization for Scientific Research (CW-NWO). J. Piris and Dr. B. R. Wegewijs (IRI) are gratefully acknowledged for their experimental contribution.

Supporting Information Available: The synthetic procedures for the preparation of **2e** and D−B−A compounds **D-[3*π*3*π*3*π*3]A**, **D[7*π*3]A**, **D[11]A**, and **D[3*π*7]A**. Deconvoluted fluorescence spectra of **D[3*π*3]A** in cycohexane and of **D[7*π*3]-A** in diethyl ether and di-*n*-butyl ether (PDF). This information is available free of charge via the Internet at http://pubs.acs.org.

References and Notes

(1) Wasielewski, M. R. *Chem. Rev.* **1992**, *92*, 435−461.

(2) Oevering, H.; Paddon-Row: M. N.; Heppener, M.; Oliver, A. M.; Cotsaris, E.; Verhoeven, J. W.; Hush, N. S. *J. Am. Chem. Soc.* **1987**, *109*, 3258−3269.

(3) Bolton, J. R., Mataga, N.,McLendon, G., Eds. *Electron Transfer in Inorganic, Organic, and Biological Systems*; Advances in Chemistry Series 228; American Chemical Society: Washington, DC, 1991.

(4) Barbara, P. F.; Meyer, T. J.; Ratner, M. A. *J. Phys. Chem.* **1996**, *100*, 13148−13168.

(5) McConnell, H. M. *J. Chem. Phys.* **1961**, *35*, 508−515.

(6) Friesner, R. A.; Won, Y. *Biochim. Biophys. Acta* **1989**, *977*, 99−122.

(7) Tsue, H.; Imahori, H.; Kaneda, T.; Tanaka, Y.; Okada, T.; Tamaki, K.; Sakata, Y. *J. Am. Chem. Soc.* **2000**, *122*, 2279−2288.

(8) Miller, S. E.; Lukas, A. S.; Marsh, E.; Bushard, P.; Wasielewski, M. R. *J. Am. Chem. Soc.* **2000**, *122*, 7802−7810.

(9) Bixon, M.; Jortner, J. *J. Chem. Phys.* **1997**, *107*, 5154−5170.

(10) Sumi, H.; Kakitani, T. *Chem. Phys. Lett.* **1996**, *252*, 85−93.

(11) Hoogesteger, F. J.; Havenith, R. W. A.; Zwikker, J. W.; Jenneskens, L. W.; Kooijman, H.; Veldman, N.; Spek, A. L. *J. Org. Chem.* **1995**, *60*, 4375−4384.

(12) Marsman, A. W.; Havenith, R. W. A.; Bethke, S.; Jenneskens, L. W.; Gleiter, R.; van Lenthe, J. H.; Lutz, M.; Spek, A. L. *J. Org. Chem.* **2000**, *65*, 4584−4592.

(13) Marsman, A. W.; Havenith, R. W. A.; Bethke, S.; Jenneskens, L. W.; Gleiter, R.; van Lenthe, J. H. *Eur. J. Org. Chem.* **2000**, 2629−2641.

(14) Bakkers, E. P. A. M.; Roest, A. L.; Marsman, A. W.; Jenneskens, L. W.; de Jong-van Steensel, L. I.; Kelly, J. J.; Vanmaekelbergh, D. *J. Phys. Chem. B* **2000**, *104*, 7266−7272.

(15) Bakkers, E. P. A. M.; Marsman, A. W.; Jenneskens, L. W.; Vanmaekelbergh, D. *Angew. Chem., Int. Ed. Engl.* **2000**, *39*, 2297−2299.

(16) Holmlin, R. E.; Ismagilov, R. F.; Haag, R.; Mujica, V.; Ratner, M. A.; Rampi, M. A.; Whitesides, G. M. *Angew. Chem., Int. Ed. Engl.* **2001**, *40*, 2316−2320.

(17) Davis, W. B.; Svec, W. A.; Ratner, M. A.; Wasielewski, M. R. *Nature* **1998**, *396*, 60−63.

(18) Hoogesteger, F. J.; van Walree, C. A.; Jenneskens, L. W.; Roest, M. R.; Verhoeven, J. W.; Schuddeboom, W.; Piet, J. J.; Warman, J. M. *Chem. Eur. J.* **2000**, *6*, 2948−2959.

(19) For a related example see: Willemse, R. J. Photoinduced Electron Transfer in Donor−Acceptor Systems with Redox-Active Bridges. Thesis, University of Amsterdam, Amsterdam, The Netherlands, 1997.

(20) Wegewijs, B.; Hermant, R. M.; Verhoeven, J. W.; Kunst, A. G. M.; Rettschnick, R. P. H. *Chem. Phys. Lett.* **1987**, *140*, 587−590.

(21) Lauteslager, X. Y.; van Stokkum, I. H. M.; van Ramesdonk, H. J.; Brouwer, A. M.; Verhoeven, J. W. *J. Phys. Chem. A* **1999**, *103*, 653−659.

(22) Wegewijs, B.; Verhoeven, J. W. Long-Range Charge Separation in Solvent-Free Donor-Bridge-Acceptor Systems. In *Electron-Transfer from Isolated Molecules to Biomolecules, Part One*; Jortner, J.; Bixon, M., Eds.; Advances in Chemical Physics 106; John Wiley & Sons: New York, 1999.

(23) Schuddeboom, W.; Scherer, T.; Warman, J. M.; Verhoeven, J. W. *J. Phys. Chem.* **1993**, *97*, 13092−13098.

(24) Hoogesteger, F. J. Oligo(Cyclohexylidenes), Development of Novel Functional and Organized Materials. Thesis, Utrecht University, Utrecht, The Netherlands, 1996.

(25) Sánchez, I. H.; Ortega, A.; García, G.; Larraza, M. I.; Flores, H. J. *Synth. Commun.* **1985**, *15*, 141−149.

(26) Wells, A. P.; Kitching, W. *J. Chem. Soc., Perkin Trans. 1* **1995**, 527−535.

(27) Trost, B. M.; Tamaru, Y. *J. Am. Chem. Soc.* **1977**, *99*, 3101−3113.

(28) Paddon-Row, M. N. *Acc. Chem. Res.* **1994**, *27*, 18−25.

(29) Shephard, M. J.; Paddon-Row, M. N. *J. Phys. Chem. A* **2000**, *104*, 11628−11635.

(30) Paulson, B.; Pramod, K.; Eaton, P.; Closs, G.; Miller, J. R. *J. Phys. Chem.* **1993**, *97*, 13042−13045.

(31) Pasman, P.; Koper, N. W.; Verhoeven, J. W. *Recl. Trav. Chim. Pays-Bas* **1982**, *101*, 363−364.

(32) Closs, G. L.; Calcaterra, L. T.; Green, N. J.; Penfield, K. W.; Miller, J. R. *J. Phys. Chem.* **1986**, *90*, 3673−3683.

(33) Asveld, E. W. H.; Kellogg, R. M. *J. Org. Chem.* **1982**, *47*, 1250−1257.

(34) Oosterbaan, W. D.; Koeberg, M.; Piris, J.; Havenith, R. W. A.; van Walree, C. A.; Wegewijs, B. R.; Jenneskens, L. W.; Verhoeven, J. W. *J. Phys. Chem. A* **2001**, *105*, 5984−5989.

(35) Oosterbaan, W. D.; Havenith, R. W. A.; van Walree, C. A.; Jenneskens, L. W.; Gleiter, R.; Kooijman, H.; Spek, A. L. *J. Chem. Soc., Perkin Trans. 2* **2001**, 1066−1074.

(36) Hoogesteger, F. J.; van Lenthe, J. H.; Jenneskens, L. W. *Chem. Phys. Lett.* **1996**, *259*, 178−184.

(37) Havenith, R. W. A.; van Lenthe, J. H.; Jenneskens, L. W.; Hoogesteger, F. J. *Chem. Phys.* **1997**, *225*, 139−152.

(38) Pasman, P.; Rob, F.; Verhoeven, J. W. *J. Am. Chem. Soc.* **1982**, *104*, 5127−5133.

(39) Hermant, R. M.; Bakker, N. A. C.; Scherer, T.; Krijnen, B.; Verhoeven, J. W. *J. Am. Chem. Soc.* **1990**, *112*, 1214−1221.

(40) Scherer, T.; Hielkema, W.; Krijnen, B.; Hermant, R. M.; Eijckelhoff, C.; Kerkhof, F.; Ng, A. K. F.; Verleg, R.; van der Tol, E. B.; Brouwer, A. M.; Verhoeven, J. W. *Recl. Trav. Chim. Pays-Bas* **1993**, *112*, 535−548.

(41) Excitation spectra suggest that the remaining "local emission" is, at least in part, due to emission from molecules which lack the acceptor and are present as a minor impurity.

(42) Marcus, R. A. *J. Phys. Chem.* **1989**, *93*, 3078−3086.

(43) It should be noted that for the fitting procedure the experimental spectra $I(\lambda)$ were converted to a cm^{-1} scale without correction for the intensity (which is usually done via $I(\nu) = \lambda^2 I(\lambda)$, see Lakowicz, J. R. *Principles of Fluorescence Spectroscopy*; Plenum Press: New York, 1983; Chapter 2) since this correction will shift the maxima. Without correction the fitted maxima ν_{max} in cm^{-1} are directly comparable to experimental maxima ν_f.

(44) Fraser, R. D. B.; Suzuki, E. *Anal. Chem.* **1969**, *41*, 37−39.

(45) Variation of the band widths $\Delta\nu$ in the range $(4.75-5.50) \times 10^3$ cm^{-1} did not result in shifts of maxima ν_{max} larger than ca. 300 cm^{-1} relative to the values in Table 4.

(46) The contribution of a small amount of CCT emission in these solvents cannot be excluded.

(47) Beens, H.; Knibbe, H.; Weller, A. *J. Chem. Phys.* **1967**, *47*, 1183−1184.

(48) Lippert, E. *Z. Elektrochem.* **1957**, *61*, 962−975.

(49) Here it is assumed that ρ^3 varies as the product of R_c and the molecule's cross section and that μ_e^2 varies as the product of R_c^2 and e^2.

(50) Shida, T. *Electronic Absorption Spectra of Radical Ions*; Physical Sciences Data 34; Elsevier: Amsterdam, 1988.

(51) Roest, M. R.; Lawson, J. M.; Paddon-Row: M. N.; Verhoeven, J. W. *Chem. Phys. Lett.* **1994**, *230*, 536−542.

(52) The fluorescence maxima in THF were omitted in these fits. Their position and the polar nature of the solvent are in line with the occurrence of ECT fluorescence.

(53) A comparison with **D[3π3]A** instead of **D[3]A** yields distances of 2.1−2.3 Å.

(54) One of the referees remarked that the energy of a virtual state is not solvent dependent since there is no driving force for solvent alignment. However, in the (relaxed) CCT state, solvent reorganization has already occurred around the acceptor and this will also have a stabilizing effect on the virtual $[3\pi^{\bullet+}3]A^{\bullet-}$ state. Thus, the $[3\pi^{\bullet+}3]A^{\bullet-}$ level is also solvent dependent.

(55) van Walree, C. A.; Roest, M. R.; Schuddeboom, W.; Jenneskens, L. W.; Verhoeven, J. W.; Warman, J. M.; Kooijman, H.; Spek, A. L. *J. Am. Chem. Soc.* **1996**, *118*, 8395−8407.

(56) van Dijk, S. I.; Wiering, P. G.; van Staveren, R.; van Ramesdonk, H. J.; Brouwer, A. M.; Verhoeven, J. W. *Chem. Phys. Lett.* **1993**, *214*, 502−506.

(57) Wasielewski, M. R.; Niemczyk, M. P.; Johnson, D. G.; Svec, W. A.; Minsek, D. W. *Tetrahedron* **1989**, *45*, 4785−4806.

(58) de Haas, M. P.; Warman, J. M. *Chem. Phys.* **1982**, *73*, 35−53.

(59) Schuddeboom, W. Photophysical Properties of Opto-Electric Molecules Studied by Time-Resolved Microwave Conductivity. Thesis, Delft University of Technology, Delft, The Netherlands, 1994.

(60) Weller, A. *Z. Phys. Chem., Neue Folge* **1982**, *133*, 93−98.

(61) Rehm, D.; Weller, A. *Ber. Bunsen-Ges. Phys. Chem.* **1969**, *73*, 834−839.

(62) For the absorption spectrum, this is a plot of $\epsilon(\nu)/\nu$ vs. ν. For fluorescence spectra the wavenumber dependency of the Einstein coefficient of spontaneous emission has to be taken into account and the corrected spectrum is represented by $I(\nu)/\nu^3$ vs ν, where $I(\nu) = I(\lambda)\lambda^2$.

(63) Bolton, J. R.; Archer, M. D. Basic Electron-Transfer Theory. In *Advances in Chemistry Series 228*: *Electron Transfer in Inorganic, Organic, and Biological Systems*; Bolton, J. R., Mataga, N., McLendon, G., Eds.; American Chemical Society: Washington, DC, 1991.

(64) Marcus, R. A.; Sutin, N. *Biochim. Biophys. Acta* **1985**, *811*, 265−322.

(65) de Rege, P. J. F.; Williams, S. A.; Therien, M. J. *Science* **1995**, *269*, 1409−1413.

(66) Kroon, J.; Verhoeven, J. W.; Paddon-Row: M. N.; Oliver, A. *Angew. Chem., Int. Ed. Engl.* **1991**, *30*, 1358−1361.

(67) Brandsma, L.; Verkruijsse, H. D. *Preparative Polar Organometallic Chemistry 1*; Springer-Verlag: Berlin, 1987; pp 7−8.

(68) Eaton, D. F. *Pure Appl. Chem.* **1988**, *60*, 1107−1114.

(69) Willemse, R. J.; Piet, J. J.; Warman, J. M.; Hartl, F.; Verhoeven, J. W.; Brouwer, A. M. *J. Am. Chem. Soc.* **2000**, *122*, 3721−3730.

(70) Marsman, A. W. Functionalized Oligo(Cyclohexylidenes). Semi-rigid Molecular Rods for Crystal Engineering, Through-Bond Orbital Interactions and Self-Assembly. Thesis, Utrecht University, Utrecht, The Netherlands, 1999, Chapter 8.